Synthesis and release behavior of layered double hydroxides – carbamazepine composites

Maria Peralta
Centro de Investigación y Tecnología Química - CONICET - UTN
Silvia Mendieta (smendieta@frc.utn.edu.ar)
Centro de Investigación y Tecnología Química - CONICET - UTN
Ivana Scolari
Unidad de Investigación y Desarrollo en Tecnología Farmacéutica – CONICET - UNC
Gladys Granero
Unidad de Investigación y Desarrollo en Tecnología Farmacéutica – CONICET - UNC
Monica Crivello
Centro de Investigación y Tecnología Química - CONICET - UTN

Research Article

Keywords: Layered Double Hydroxides, Carbamazepine, Drug delivery, neutral drugs, clay

Posted Date: November 24th, 2020

DOI: https://doi.org/10.21203/rs.3.rs-112227/v1

Synthesis and release behavior of layered double hydroxides – carbamazepine composites

Peralta, Ma. F.[1,2]; Mendieta, S. N.[1,*]; Scolari, I. R.[2]; Granero, G. E.[2]; Crivello, M. E.[1,*]

[1] Centro de Investigación y Tecnología Química – CONICET – Universidad Tecnológica Nacional, Regional Córdoba, Córdoba, Argentina

[2] Unidad de Investigación y Desarrollo en Tecnología Farmacéutica – CONICET – Universidad Nacional de Córdoba; Departamento de Ciencias Farmacéuticas, Universidad Nacional de Córdoba, Córdoba, Argentina.

[*] Corresponding author: SM: smendieta@frc.utn.edu.ar Maestro López esq. Cruz Roja Argentina, S/N, X5016ZAA, Córdoba, Argentina. Phone: +549-0351-4690585-13

MC: mcrivello@frc.utn.edu.ar Maestro López esq. Cruz Roja Argentina, S/N, X5016ZAA, Córdoba, Argentina. Phone: +549-0351-4690585-13

Abstract

Carbamazepine (CBZ) was incorporated into Layered Double Hydroxides (LDH) to be used as controlled drug delivery in solid tumors. CBZ has a formal charge of 0, which implies a challenge to be incorporated in the anionic clay. Aiming to overcome this problem, CBZ was first incorporated in micelles of sodium cholate (SC), a surfactant with negative charge. CBZ in SC micelles and, for comparison, free CBZ were incorporated in LDH by reconstruction method. It was found that resultant nano-composites had similar CBZ encapsulation efficiency, around 75 %, but drug release in simulated body fluid (pH 7.4) and acetate buffer (pH 4.8) was efficient only with the LDH-CBZ sample. CBZ dimensions were measured with Chem3D and, according to the basal spacing obtained from X rays patterns, it can arrange as monolayer with the long axis parallel to the LDH layers. Fourier Transform Infrared Spectroscopy confirmed the incorporation of the drug. Thermogravimetric analyses showed and enhanced thermal stability for CBZ. These results have interesting implications since they increase the spectrum of LDH application as controlled drug delivery to a large number of non-ionic drugs, without the addition of other components.

Key words

Layered Double Hydroxides, Carbamazepine, Drug delivery, neutral drugs, clay

Introduction

Layered Double Hydroxides (LDH) are inorganic solids composed of metal cationic layers and inter-lamellar spaces filled with negative ions. In the last years, LDH have gained interest as carriers for anionic drugs, which replace the ions between layers [1–4]. Most anti-tumor drugs are systemically administered, and this produces several side effects all the way, until the drug reaches the target site. LDH could solve this problem by protecting the drug during blood circulation (pH 7.4) and releasing it inside the tumor cells (pH 4.8). This is possible because, at neutral pH, LDH are stable which maintain the encapsulated drugs in the interlayers of their lamellar structure; in this case, the release of the molecules may occur only through diffusion. At acidic pH, below 5, LDH dissolves, their structure is broken and the encapsulated molecules are released quickly, first through diffusion and then by the removal of LDH layers [5–7].

LDH have the advantages of been homogeneous mixtures of oxides with very small crystal size, from 20 to 200 nm, depending on temperature and time of synthesis; these nano-sizes are fundamental for drug delivery systems intended to systemic administration. LDH are also stable to thermal treatments and they have memory effect, which allows the reconstruction of the original lamellar structure when contacting the metal oxides with water solutions containing various anions [1]. LDH are usually prepared by co-precipitation of the metal salts solutions, in a controlled pH and temperature. Metals form a brucite like layer while water and anions form the interlayers. The drugs can be incorporated by ion exchange, which necessary implies anionic molecules that replaces the anions of the interlayers, or by reconstruction, which uses the recovery memory effect of LDH. In the last case, layers are first converted to metal oxides by calcination and then reconstructed in an aqueous medium containing the drug. This may be a way to incorporate non-ionic molecules in the interlayers.

Carbamazepine (CBZ) is an anticonvulsant drug with a formal charge of 0. It has shown efficacy against some solid cancer cell lines, like SK-BR-3 and MDA-MB-231 corresponding to human breast cancer [8]. In SW480 cell line, corresponding to human colon adenocarcinoma, CBZ showed a 50 % inhibitory concentration of 5 μM [9]. It also produces alterations in red blood cells [10].

CBZ is poorly soluble in water and many authors have increased the solubility through its complexation with D-gluconolactone [11], polymers [12], cyclodextrins [13] or surfactants like sodium lauryl sulfate and Tween 80 [14].

Sodium cholate (SC) is a bill salt surfactant with negative charge that forms micelles at critical micelle concentration. In the process, the drugs that are in the medium can be encapsulated into the micelles. SC can be used to enhance solubility of drugs [15] or to give negative charge [5].

In this work, CBZ was incorporated into LDH composed of Mg-Al-NO_3, in micelles of SC by using different methods: ionic exchange and reconstruction. The reconstruction method was also performed with free CBZ for comparison purposes. Different techniques were applied to characterize the systems and to determine their efficacy as drug carriers.

Results

The XRD patterns of LDH sample exhibited characteristic diffraction peaks (Figure 1). The basal spacing (d_{003}) corresponding to NO_3^- ions was 7.8 Å. The pattern of LDH-CBZ was very similar to that of the LDH, with good crystallized structure and a basal spacing of 7.8 Å. CBZ dimensions were measured with Chem3D 18.0 (Perkin Elmer) and are shown in Figure 2 a. Figure 2 b shows the way that CBZ can accommodate into the LDH.

In the samples containing SC, the basal spacing (d_{003}) corresponding to the first peak, increased to 11.5 Å and 17.3 Å in LDH-CBZ-SC60 and LDH-CBZ-SC60(IE) respectively (Figure 1). On the other hand, spectra of LDH-CBZ-SC60(IE) between 60º and 63º showed a very disordered structure. The probable organization of CBZ and SC in the LDH is shown in Figure 2 c, taking into account the size of SC molecules (4.68 Å in thickness and 15 Å in length, measured with Chem3D). The diffractogram of LDH-CBZ-SC60 sample also shows some peaks characteristics of pure CBZ, which indicates that some drug remained in the surface of the LDH.

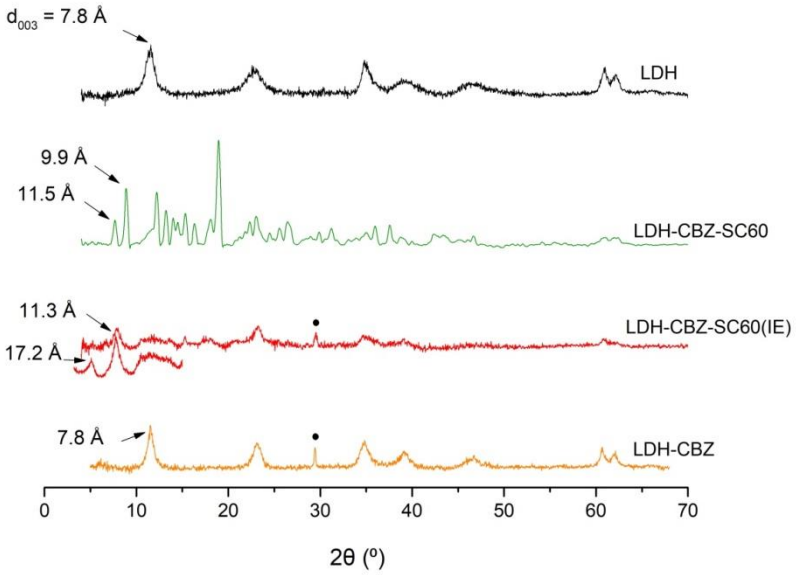

Figure 1 Powder X-ray diffraction patterns of LDH and CBZ-LDH composites. ● Indicates peaks of sodium nitrate salt that remains in the sample.

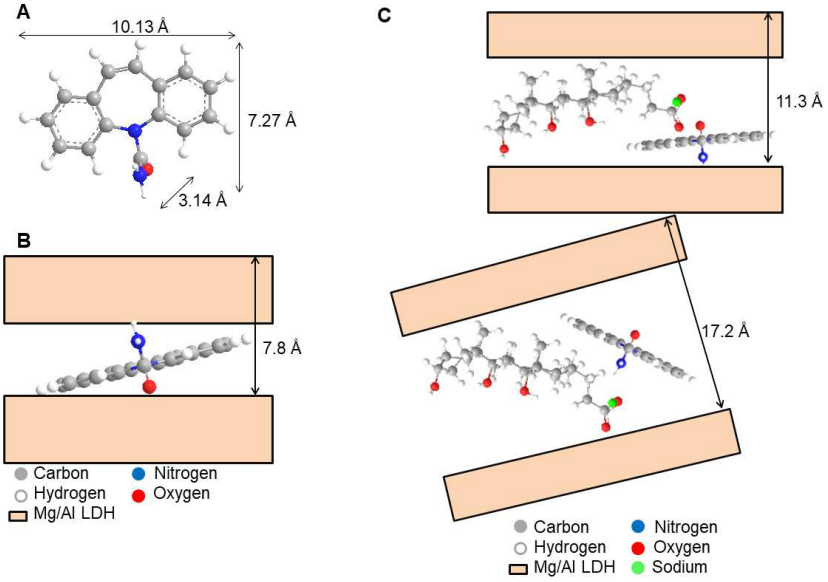

Figure 2 a) CBZ dimensions calculated with Chem3D. **b)** Probable CBZ orientation in LDH-CBZ. **c)** Probable CBZ and SC orientation in LDH-CBZ-SC60(IE).

The characteristic transmittance peaks of CBZ, at 1597 cm^{-1} (N-H deformation) and 1685 cm^{-1} (C=O stretching) [23], appear in the FTIR spectrum of LDH-CBZ (Figure 3), indicating that CBZ molecules were loaded on LDH. Absorption at 1384 cm^{-1} can be assigned to the v_3 vibration of NO_3^-, which are also in the interlayers. The band at 1638 cm^{-1}, due to the bending mode of water molecules, disappears in the LDH-CBZ spectra.

The peak at 448 cm^{-1} is attributed to metal-O lattice vibrations. The spectra of the samples containing SC were difficult to analyze since the surfactant has wide and strong bands that overlap the peaks of the CBZ (Figure 3); however, the peak at 1685 cm^{-1} (C=O stretching) is detectable, which shows the presence of the drug in the composites.

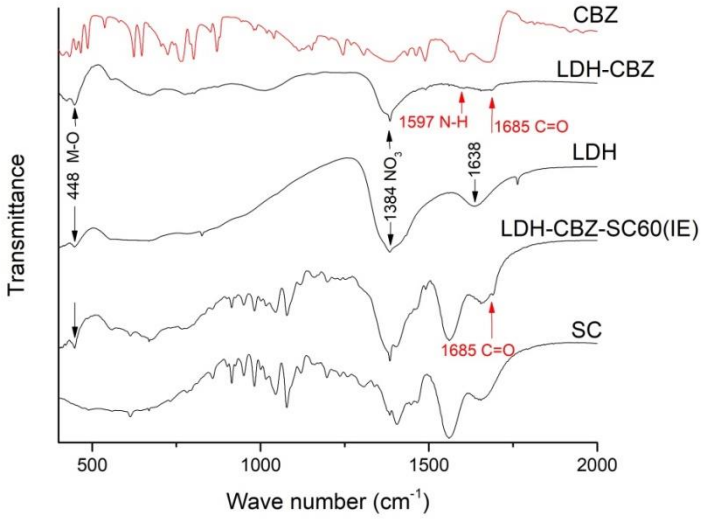

Figure 3 FTIR spectra of CBZ, SC, LDH and CBZ-LDH composites.

TEM images (Figure 4 a-d) shows the laminar structure of LDH in all the samples, with the typical thin, plate-like shape and dimensions below 100 nm (Figure 4 e). The addition of SC and CBZ did not change the dimension of the crystals although tend to agglomerate them. In the samples with SC, the ion exchange method seems better than reconstruction, since aggregates are smaller (Figure 4 c and d respectively).

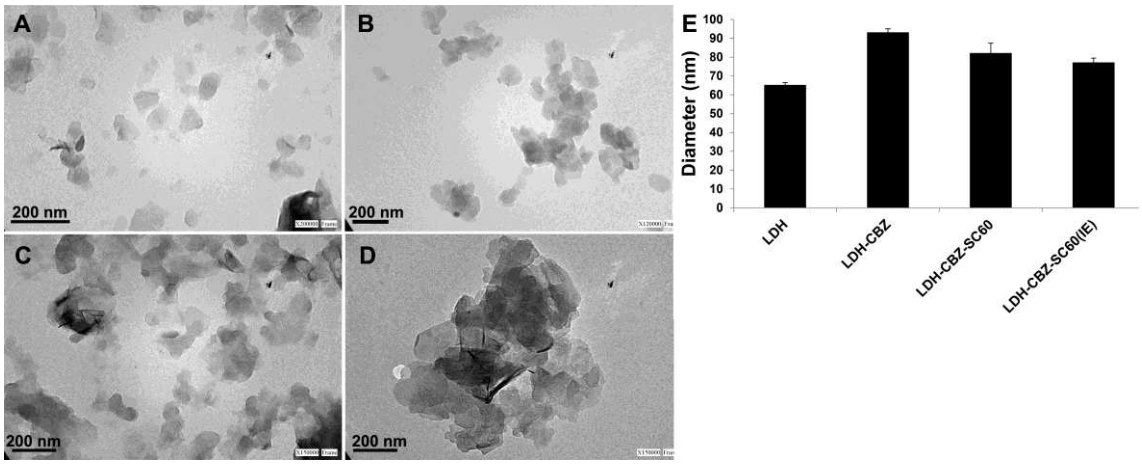

Figure 4 TEM images of a) pristine LDH, **b)** LDH-CBZ, **c)** LDH-CBZ-SC60(IE) and **d)** LDH-CBZ-SC60. **e)** Diameter of LDH in different samples measured from TEM images.

Thermal behavior of the composites was determined by TG and DTG (Figure 5). The TG curves of the samples containing SC present similar weight loss of around 70 %. In the LDH-CBZ sample, the total weight loss was only 45 %; this difference is due to the absence of SC. In the sample synthetized by reconstruction, it can be observed by DTG analyses that the first thermal event, occurred between 70-80 °C, correspond to the CBZ dehydration [24]; the transitions observed up to 170 °C are associated with the removal of the interlayer water. Finally, the last transition corresponds to SC decomposition [25]. In the LDH-CBZ-SC60(IE) sample is not possible to observe a high loss of physisorbed water, due to low moisture content present in the host LDH.

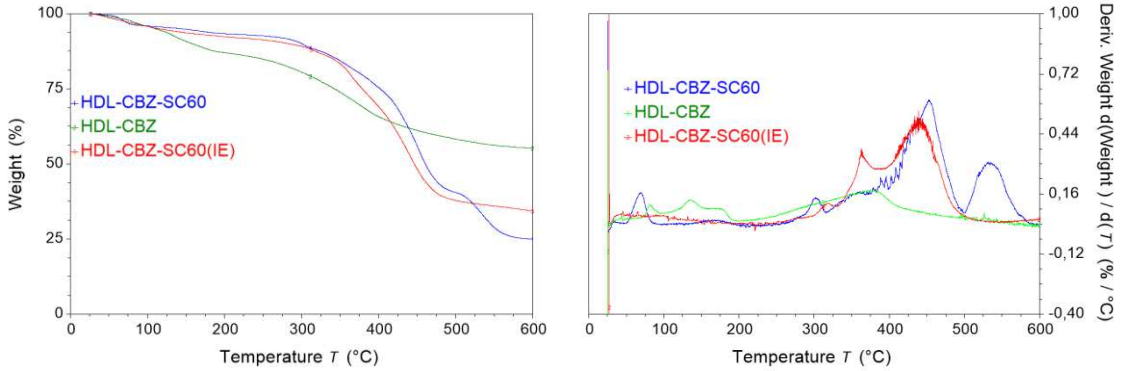

Figure 5 TG curves and DTG of composites.

Table 1 shows the results of the CBZ loading into the LDH from the different synthesis methods. EE was high in all the samples; it was similar for LDH-CBZ and LDH-CBZ-SC60 (75 %) and its value increased to 95 % in LDH-CBZ0-SC60(IE).

Table 1 CBZ loading and encapsulation efficiency in the different composites.

	CBZ loading (%)	**Encapsulation efficiency (EE) (%)**
LDH-CBZ	5.3 ± 0.6	75
LDH-CBZ-SC60	1.6 ± 0.0	75
LDH-CBZ-SC60(IE)	1.8 ± 0.2	95

Release profiles of CBZ, pure and from the different composites, are shown in Figure 6. The patterns at pH 7.4 and 4.8 cannot be directly compared because CBZ behaves differently in the two mediums, going faster to the receptor medium at pH 7.4. The statistical analysis of these results was made by comparing the CBZ release profiles of

the different systems with that one of the free drug. Table 2 shows the F1 and F2 factors, where F1<15 and F2>50 imply the release profiles are equals or similar.

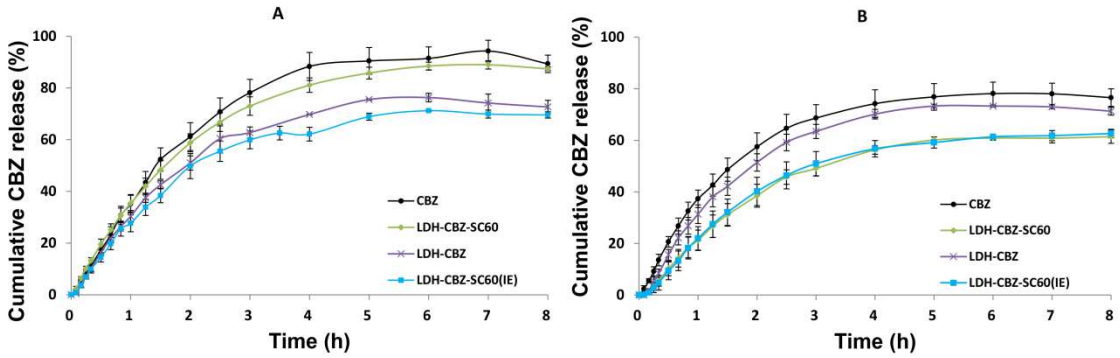

Figure 6 *In vitro* CBZ release profiles in **a)** SBF, pH 7.4 and **b)** acetate buffer, pH 4.8. CBZ solution in the respective mediums was used as reference (mean ± SD, n = 3).

Table 2I Statistical analysis of CBZ release profiles. Comparisons were made for each system developed with respect to the free drug.

	SBF (pH 7.4)			Acetate buffer (pH 4.8)		
	F1	**F2**	**Interpretation**	**F1**	**F2**	**Interpretation**
LDH-CBZ	17.2	48.2	Different curves	10.7	64.9	Same curves
LDH-CBZ-SC60	5.5	72.9	Same curves	30.5	41.5	Different curves
LDH-CBZ-SC60(IE)	22.9	42.3	Different curves	29.9	42.1	Different curves

The diffusion release mechanism of CBZ from the LDH was verified by testing for linearity between $-\ln (1-Q_t/Q_0)$ and $t^{0,65}$, according to Bhaskar equations (Table 3). CBZ may have been released from LDH at pH 7.4 by controlled diffusion, since the Bhaskar method showed linearity with an R^2 of 0.9953. The correlation coefficient for the experiment at pH 4.8 was also good, although a bit smaller: 0.9937. CBZ can also be released from samples with SC by diffusion (Table 4).

Table 3 Equations for fitting the data of the CBZ release.

Model	Equation	Reference
Bhaskar	$-\ln (1 - Q_t / Q_0) = 1.59 (6 / d_P)^{1.3} D^{0.65} t^{0.65}$	19

Pseudo-1st-order	$\ln (Q_e - Q_t) = \ln Q_e - K_1 t$	20
Pseudo-2nd-order	$t / Q_t = 1 / K_2 Q_e^2 + t / Q_e$	21

t = time; Q_0 = drug content at time t = 0; Q_t = drug content at any time; Q_e = drug content at equilibrium; d_p = particle diameter; D = diffusivity

Table 4 Correlation coefficient (R^2) obtained by fitting the data of the CBZ release into SBF (pH 7.4) and acetate buffer (pH 4.8).

		Bhaskar	**Parabolic diffusion**	**Pseudo-1st-order**		**Pseudo-2nd-order**
					K_1 (min^{-1})	
LDH-CBZ	pH 7.4	0.9953	0.5993	0.9950	0.6404	0.9349
	pH 4.8	0.9937	0.3500	0.9845	0.7525	0.9163
LDH-CBZ-SC60	pH 7.4	0.9896	0.7732	0.9852	0.6884	0.9815
	pH 4.8	0.9940	0.1880	0.9795	0.6540	0.4043
LDH-CBZ-SC60(IE)	pH 7.4	0.9488	0.6236	0.9881	0.6364	0.9373
	pH 4.8	0.9876	0.0548	0.9720	0.7551	0.1614

Pseudo-first-order kinetic model was evaluated by testing for linearity between ln (Q_e-Q_t) and t, according to the model equation, shown in Table 3. The rate constant K_1 was obtained from the slope of the linear plot. Pseudo-second-order kinetic model was evaluated by testing for linearity between t / Q_t and t (Table 3). Results are shown in Table 4 and Figure 7; pseudo-first-order model was the most satisfactory for describing the release kinetic processes of CBZ from the LDH-CBZ composite, with an R^2 of 0.995 and a K_1 of 0.64 min^{-1} at pH 7.4 and an R^2 of 0.985 and K_1 of 0.75 min^{-1} at pH 4.8. The samples with SC, also fitted better with pseudo-first-order kinetic model (Table 4), with R^2 between 0.969 and 0.988, than with the others one.

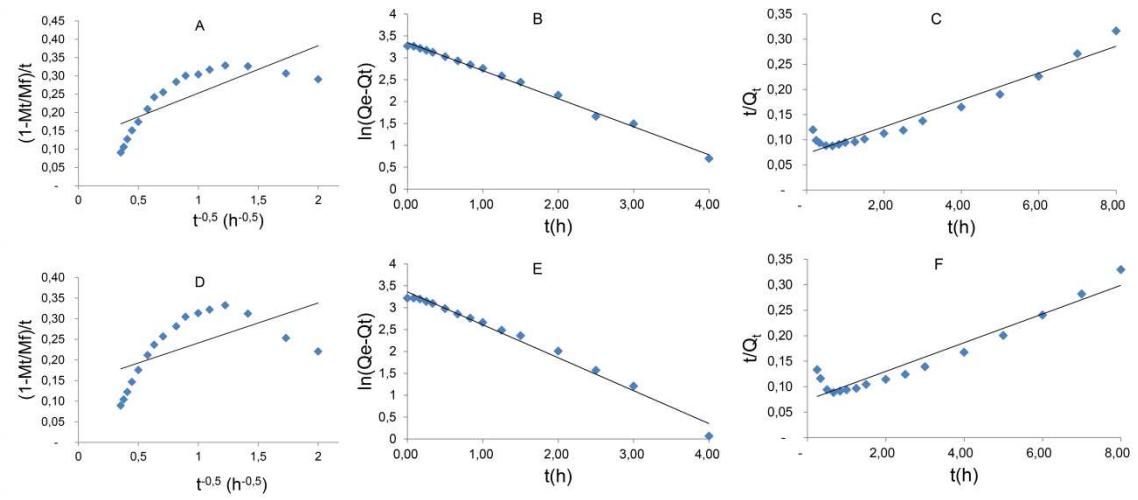

Figure 7 Fitting of the data of CBZ release from LDH-CBZ composite to parabolic diffusion (**a** and **d**), pseudo-first (**b** and **e**) and pseudo-second (**c** and **f**) order kinetics for SBF, pH 7.4 **(a-c)** and acetate buffer, pH 4.8 **(d-f)**.

Discussion

CBZ is a neutral molecule that has shown activity against some cancer cell lines. The incorporation of the drug in Hydroxides Double Layered (LDH) could avoid its side effects during blood circulation and allow its activity in the target sites. LDH are clays composed for cationic layers and stabilized with anionic molecules in the inter-laminar space. Sodium cholate (SC), an anionic surfactant, was used to facilitate CBZ incorporation into the LDH interlayers, and the free drug was incorporated for comparison.

The synthetized LDH had a well-crystallized structure. The low value observed in the inter-laminar distance may be due to the low hydration that the material presents. Other authors, who suggest that the nitrate anion accommodates itself in a parallel way to the brucite layer without widening due to the few water molecules that surround it, obtained similar data. Iyi et al reported c values between 21.6 and 22.8 Å for nitrate anions [26,27].

The structure and basal spacing of the LDH containing CBZ was very similar to that of the LDH. The very small increase in the d_{003}, can be due to the small size of the molecule (molecular size = 236 Da) [28,29], which makes it possible to stays in the interlayer without changing its initial distance. The interlayer domains contain not only anions but also water and neutral molecules [4], and the non-ionic CBZ molecules perhaps could be stabilized in the gallery of LDH because of hydrogen bonds between H of OH (from brucite-type layers) and O or N of the CBZ molecules intercalated. These results agree with that of Dong et al. [30], where the incorporation of camptothecin,

a molecule similar and slightly larger than CBZ, produced only a small increase in the interlayer space. The authors proposed that the molecules arrange as monolayers with the long axis parallel to the LDH layers. The incorporation of CBZ into the LDH was confirmed by FTIR.

In the samples containing SC, the intensity of XRD peaks decreased in comparison with those of the LDH, indicating some reductions in crystallinity following the intercalation of SC and CBZ. It also appeared a second peak that indicates two basal spacing and possible orientation of the molecules in the LDH. The basal spacing corresponding to the first peak indicates that SC was intercalated into the gallery of the LDH but not in the form of micelles.

By literature, the decomposition of pure CBZ begins at 200 °C [24]; in DTG diagrams the decomposition is not observed until 300 °C, which can be associated with the superficial CBZ observed in LDH-CBZ-SC60 by XRD. From 350 °C, the decomposition of the sheets is observed; the dihydroxylation of the lamella, decomposition and combustion of the intercalated CBZ occur together. The thermal decomposition temperature of the CBZ was strongly affected by the host layer. These results confirmed the enhanced thermal stability of the drug.

Regarding CBZ loading into the LDH, it is the percentage of CBZ in the system, and it was higher in LDH-CBZ than in the samples with SC because of the fewer components of synthesis. The encapsulation efficiency was high (75 %) and the same for the samples with and without SC when the reconstruction method was used; this indicates that SC is not necessary to incorporate along with CBZ into the LDH. The encapsulation was higher (95 %) in the sample with SC synthetized by ion exchange, but this method of synthesis is not possible to apply in the case of the uncharged free drug.

Assays of *in vitro* drug released were done in Franz Cells with SBF (pH 7.4) and Acetate buffer (pH 4.8) in order to analyze the protector roll of the nano-system developed in the blood and the drug release inside the tumor cells respectively. LHD-CBZ was the only system able to protect the drug at the pH value of the blood (pH 7.4) and release it at the pH value of the cell cytoplasm (pH 4.8). In the case of LDH-CBZ-SC60, the presence of CBZ in the surface of the LDH can explain the fast release of the drug at pH 7.4. A controlled release of CBZ was obtained with the system synthesized

by anion exchange (LDH-CBZ-SC60(IE)) at pH 7.4; however, the drug was not released at the pH of 4.8.

The release mechanism of CBZ from the LDH, studied by Bhaskar method, seems to be a controlled diffusion in all the samples. At acidic pH, diffusion is also the principal process for CBZ release, and LDH were dissolving but slowly. CBZ can also be released from samples with SC by diffusion, although, as described above, not efficiently.

The kinetics of drug release from LDH composites is usually described with pseudo-first and pseudo-second-order equations, or by parabolic diffusion [7,30,31]. The pseudo-first-order model was the most satisfactory in our systems. K_1 values confirmed the faster release of CBZ at acidic than neutral pH in LDH-CBZ samples. In the samples with SC, K_1 values also confirm the results discussed previously with CBZ release patterns. We also fitted the data with Ritger and Peppas, modified Freundlich, K-K and Higuchi models, however, they had not sufficiently good correlation coefficients.

Conclusion

Results suggest that not only ionic bonds are involved in the structure of LDH but other types of interactions also take place, which is why these systems are suitable not only for loading anionic molecules but also are promising drug delivery carriers of drugs with different charges. Neutral molecules could enter and stay in the interlayers when reconstruction method was used. LDH synthesized by the reconstruction method present a good enhanced thermal stability for CBZ and a good drug loading with an acceptable encapsulation efficiency. LDH obtained for the mentioned method were able to slowly release the CBZ at pH of 7.4 while CBZ was rapidly release at pH 4.8, thus, this composite system may be a promising drug carrier system for systemic administration of drugs targeted to intracellular sites, like anti-cancerogenic ones.

Materials and Methods

Materials

Carbamazepine (USP grade, Parafarm) was from Saporiti, Argentina. Sodium cholate and $Al(NO_3)_2 \cdot 9H_2O$ (98 %) were from Sigma Aldrich, St. Louis, USA. $Mg(NO_3)_2 \cdot 6H_2O$ (98 %) and NaOH (97 %) from Biopack and ethanol (absolute grade) from Sintorgan®.

Synthesis of composites

LDH were prepared by co-precipitation from Mg and Al nitrates. Two aqueous solutions of $Mg(NO_3)_2 \cdot 6H_2O$ (0.6 M) and $Al(NO_3)_2 \cdot 9H_2O$ (0.3 M) were prepared in 25 mL of decarbonated water, with a relationship of $M^{2+}/M^{3+} = 2$. The solutions were added at a rate of 1 mL/min to 20 mL of decarbonated water, under permanent magnetic stirring. The coprecipitation was carried out at 70 ^{0} C under nitrogen atmosphere, to avoid the incorporation of CO_2. The pH was maintained at 10.0 ± 0.2 by adding NaOH 2 M. The resulting suspension was stirred for 48 h under nitrogen atmosphere. The product was centrifuged and washed with decarbonated water until pH 7, and finally dried at room temperature. For reconstruction method drug loading, LDH were calcined at 450 ^{0} C for 9 h and stored at 120 °C.

The sample LDH-CBZ was prepared by the reconstruction method. CBZ (1 mg) was dissolved in ethanol (1 mL); 16 mg of calcined LDH and 18 mL of decarbonated water were added to the solution and the mixture was stirred for 48 h at 40 °C, in a nitrogen atmosphere. The solvents were finally evaporated in a rotary evaporator at 60 °C and the powder resultant was recovered.

For LDH-CBZ-SC samples, CBZ was first loaded into the SC micelles. For this, CBZ (1 mg) was dissolved in ethanol (1 mL); SC (60 mg) and water (8 mL) were added to the solution and the mixture was stirred for 10 minutes under nitrogen atmosphere in order to allow ethanol evaporation. The amount of water is related to the amount of SC, in order to maintain the critical micelle concentration. 16 mg of calcined LDH and 1 mL of water were added to the suspension and the mixture was stirred for 48 h at 40 °C, in a nitrogen atmosphere. The solvents were finally evaporated and the powder resultant was recovered. Samples were called LDH-CBZ-SC60.

For comparison, LDH-CBZ-SC60(IE) was prepared by ion exchange method. The process is that of previously described but LHD was incorporated in the original slurry (1 mL) instead of calcined.

Characterization

Powder X-ray diffraction (XRD) patterns were collected on a X'Pert Pro-PANalytical diffractometer using Cu Kα radiation (λ = 1.54 Å) at a scan speed of 3^0 /min in 2θ and

step size 0.02^0 in a scan range between 2^0 and 15^0 and at a step time of 4.25 seg and step size 0.026^0 in 2θ, continuous, in a scan range between 4^0 and 70^0 .

Fourier transform infrared (FTIR) spectra were recorded on a Nicolet iS10 spectrometer at room temperature. The samples were pressed into a disc at 4 tons with KBr. The spectrum of each sample was recorded by accumulating 48 scans at 2 and 4 cm^{-1} resolution, between 400 and 4000 cm^{-1}.

Transmission electron microscopy (TEM) was performed in a JEOL JEM EXII 1200 microscope, operated at 80 kV. 0.5 mg of sample was dispersed in 4 mL of deionized water and sonicated for 30 minutes. A copper carbon grid was deposited on a small drop of the dispersion for 30 seconds and then allowed to dry. From TEM images, diameter of each LDH was determined in two perpendicular directions using Fiji Image J software. In at least 4 images of each sample, all the well visible LDH were measured.

Thermogravimetric analyses (TG) was performed by means of an automatic thermal analyzer (TA Instrument, Discovery series). Thermal analyses were conducted at a scanning rate of 10 °C/min from 25 to 600 °C. First derivative of TG (DTG) was determined with TRIOS TA Instrument software.

Carbamazepine encapsulation efficiency

The loading amount of CBZ in the LDH was determined with a Jasco V-650 UV-visible spectrophotometer. A known amount of the system was placed in a 5 mL volumetric flask and 2.5 mL of HCl 1 M solution was added to dissolve the inorganic layers. Ethanol was added to fill the balance. The concentration of CBZ in the solution was determined at 284 nm using a calibration curve of CBZ in HCl:Ethanol 1:1 v:v. The final value was an average of three independent samples. The CBZ loading was obtained according to the concentration of CBZ in the solution and the used weight of the composite sample.

The drug encapsulation efficiency (EE) was calculated with Equation (1) [16,17].

$$\mathbf{EE}\ (\%) = \frac{\mathbf{actual\ loading\ x\ 100}}{\mathbf{theoretical\ loading}} \qquad (1)$$

***In vitro* carbamazepine release**

The release of CBZ from LDH into simulated body fluid (SBF, pH 7.4, prepared as Cuello et al. [18]) and acetate buffer (pH 4.8) was achieved in vertical Franz cells under

sink conditions (10 % saturation). Each sample (equivalent to 40 µg of CBZ) was dispersed in 1 mL of the medium solution and added into the donor compartment. Receptor was filled with 9 mL of medium solution and maintained at 37 ºC under agitation. Cellulose membrane of 14 kDa (Sigma-Aldrich, USA) was used to separate both compartments. 1 mL of sample was taken from receptor medium at different times and replaced by fresh medium. The accumulated amount of CBZ released was measured in the UV-visible spectrophotometer (Agilent Technologies Cary 60 UV-Vis®) at 284 nm. Calibration curves in the respective mediums were used for CBZ concentrations measurements.

From CBZ release patterns, molecule diffusion control was studied with Bhaskar method [19].

Release kinetics were studied with pseudo-first [20] and pseudo-second-order [21] kinetic models, and with parabolic diffusion, Ritger and Peppas, modified Freundlich, K-K and Higuchi models.

Statistical analysis

Difference factor (F1) and similarity factor (F2) were used to compare CBZ release profiles, according to Moore and Flanner [22]. The difference factor is a measurement of the relative error between the two curves (Equation (2)).

$$\mathbf{F1} = \frac{\sum_{t=1}^{n}|Rt-Tt|}{\sum_{t=1}^{n} Rt}\mathbf{x\ 100} \qquad (2)$$

Where n is the number of time points, Rt is the release value of the reference (pure CBZ) at the time t, and Tt is the release value of the test at time t.

The F2 is a measurement of the similarity in the percent release between the curves (Equation (3)).

$$\mathbf{F2 = 50\ x\ log\left(\left[1 + (1/n)\sum_{t=1}^{n}(Rt - Tt)^2\right]^{-0.5}\ x\ 100\right)} \qquad (3)$$

For curves to be considered similar, F1 value should be close to 0 (up to 15) and F2 value should be close to 100 (greater than 50).

Acknowledgments

The authors would like to thank Consejo Nacional de Investigaciones Cientificas y Técnicas (CONICET), Universidad Tecnológica Nacional (UTN) and Universidad Nacional de Córdoba (UNC) for their financial support. They would like to thank Norma Graciela Maggia and the Thermal Analysis Laboratory, from UNITEFA-CONICET-UNC.

References

1. Cavani, F., Trifirò, F. & Vaccari, A. Hydrotalcite-type anionic clays: Preparation, properties and applications. *Catal. Today* **11**, 173–301 (1991).

2. Ambrogi, V., Fardella, G., Grandolini, G. & Perioli, L. Intercalation compounds of hydrotalcite-like anionic clays with antiinflammatory agents--I. Intercalation and in vitro release of ibuprofen. *Int. J. Pharm.* **220**, 23–32 (2001).

3. Mohanambe, L. & Vasudevan, S. Anionic Clays Containing Anti-Inflammatory Drug Molecules: Comparison of Molecular Dynamics Simulation and Measurements. *J. Phys. Chem. B* **109**, 15651–15658 (2005).

4. He, J. *et al.* Preparation of Layered Double Hydroxides. in *Structure and Bonding* 119: 89-119 (2006). doi:10.1007/430_006

5. Tyner, K. M., Schiffman, S. R. & Giannelis, E. P. Nanobiohybrids as delivery vehicles for camptothecin. *J. Control. Release* **95**, 501–514 (2004).

6. Barahuie, F., Hussein, M. Z., Gani, S. A., Fakurazi, S. & Zainal, Z. Synthesis of protocatechuic acid-zinc/aluminium-layered double hydroxide nanocomposite as an anticancer nanodelivery system. *J. Solid State Chem. Fr.* **221**, 21–31 (2015).

7. Hasan, S. *et al.* Controlled-release formulation of antihistamine based on cetirizine zinc-layered hydroxide nanocomposites and its effect on histamine

release from basophilic leukemia (RBL-2H3) cells. *Int. J. Nanomedicine* **7**, 3351–3363 (2012).

8. Meng, Q. *et al.* Carbamazepine promotes Her-2 protein degradation in breast cancer cells by modulating HDAC6 activity and acetylation of Hsp90. *Mol. Cell. Biochem.* **348**, 165–171 (2011).

9. Akbarzadeh, L., Moini Zanjani, T. & Sabetkasaei, M. Comparison of Anticancer Effects of Carbamazepine and Valproic Acid. *Iran. Red Crescent Med. J.* **18**, e37230–e37230 (2016).

10. Ficarra, S. *et al.* Antiepileptic carbamazepine drug treatment induces alteration of membrane in red blood cells: Possible positive effects on metabolism and oxidative stress. *Biochimie* **95**, 833–841 (2013).

11. Moradiya, H. G., Nokhodchi, A., Bradley, M. S. A., Farnish, R. & Douroumis, D. Increased dissolution ratess of carbamazepine - gluconolactone binary blends processed by hot melt extrudion. *Pharm. Dev. Technol.* 1–8 (2015).

12. Moneghini, M., Voinovich, D., Perissutti, B. & Princivalle, F. Action of Carriers on Carbamazepine Dissolution. *Pharm. Dev. Technol.* **7**, 289–296 (2002).

13. Medarević, D., Kachrimanis, K., Djurić, Z. & Ibrić, S. Influence of hydrophilic polymers on the complexation of carbamazepine with hydroxypropyl-β-cyclodextrin. *Eur. J. Pharm. Sci. Off. J. Eur. Fed. Pharm. Sci.* **78**, 273–285 (2015).

14. Li, M., Qiao, N. & Wang, K. Influence of sodium lauryl sulfate and tween 80 on carbamazepine-nicotinamide cocrystal solubility and dissolution behaviour. *Pharmaceutics* **5**, 508–524 (2013).

15. Rosoff, M. & Serajuddin, A. T. M. Solubilization of diazepam in bile salts and in sodium cholate-lecithin-water phases. *Int. J. Pharm.* **6**, 137–146 (1980).

16. Ambrogi, V. *et al.* Eudragit® and hydrotalcite-like anionic clay composite system for diclofenac colonic delivery. *Microporous Mesoporous Mater.* **115**, 405–415 (2008).

17. Pan, D., Zhang, H., Zhang, T. & Duan, X. A novel organic–inorganic microhybrids containing anticancer agent doxifluridine and layered double hydroxides: Structure and controlled release properties. *Chem. Eng. Sci.* **65**, 3762–3771 (2010).

18. Cuello, N. I. *et al.* Drug release profiles of modified MCM-41 with superparamagnetic behavior correlated with the employed synthesis method. *Mater. Sci. Eng. C* **78**, 674–681 (2017).

19. Bhaskar, R., Murthy, R. S. R., Miglani, B. D. & Viswanathan, K. Novel method to evaluate diffusion controlled release of drug from resinate. *Int. J. Pharm.* **28**, 59–66 (1986).

20. Lagergren, S. Zur theorie der sogenannten adsorption geloster stoffe. *Bih. till K. Sven. Vetenskapsakademiens, Handl.* **24**, 1–39 (1898).

21. Ho, Y. S. & McKay, G. Pseudo-second order model for sorption processes. *Process Biochem.* **34**, 451–465 (1999).

22. Moore, J. W. & Flanner, H. H. Mathematical comparison of dissolution profiles. *Pharm. Technol.* **20**, 64–74 (1996).

23. Hardikar, S., Bhosale, A., Vanave, S. & Kamathe, B. PREPARATION AND

EVALUATION OF CO-CRYSTALS OF CARBAMAZEPINE WITH GLUCOMANNAN. *Int. J. Pharm. Pharm. Sci.* **9**, (2017).

24. Pinto, M. A. L., Ambrozini, B., Ferreira, A. P. G. & Cavalheiro, É. T. G. Thermoanalytical studies of carbamazepine: Hydration/dehydration, thermal decomposition, and solid phase transitions. *Brazilian J. Pharm. Sci.* **50**, 877–884 (2014).

25. Ramalingam, P., Pusuluri, S. T., Periasamy, S., Veerabahu, R. & Kulandaivel, J. Role of deoxy group on the high concentration of graphene in surfactant/water media. *RSC Adv.* **3**, 2369–2378 (2013).

26. Jobbágy, M. & Iyi, N. Interplay of Charge Density and Relative Humidity on the Structure of Nitrate Layered Double Hydroxides. *J. Phys. Chem. C* **114**, 18153–18158 (2010).

27. Iyi, N., Fujii, K., Okamoto, K. & Sasaki, T. Factors influencing the hydration of layered double hydroxides (LDHs) and the appearance of an intermediate second staging phase. *Appl. Clay Sci.* **35**, 218–227 (2007).

28. Yu, A. S. L. *et al.* Dialysis and extracorporeal therapies. in *Brenner and Rector's The Kidney* (2015).

29. Klein, P. & Tolbert, D. Intravenous carbamazepine: a new formulation of a familiar drug. *Expert Rev. Neurother.* **17**, 851—860 (2017).

30. Dong, L., Yan, L., Hou, W.-G. & Liu, S.-J. Synthesis and release behavior of composites of camptothecin and layered double hydroxide. *J. Solid State Chem.* **183**, 1811–1816 (2010).

31. Liu, C.-X., Hou, W.-G., Li, Y. & Li, L.-F. Synthesis and Characterization of Camptothecin Intercalated into Mg/Al Layered Double Hydroxide. *Chinese J. Chem.* **26**, 1806–1810 (2008).

Author contributions

MFP and SNM wrote the main manuscript, RIS prepared Figure 6. All authors reviewed the manuscript.

Additional information

There are no conflicts of interest to declare.

Legends

Figure 1 Powder X-ray diffraction patterns of LDH and CBZ-LDH composites. ● Indicates peaks of sodium nitrate salt that remains in the sample.

Figure 2 a) CBZ dimensions calculated with Chem3D. **b)** Probable CBZ orientation in LDH-CBZ. **c)** Probable CBZ and SC orientation in LDH-CBZ-SC60(IE).

Figure 3 FTIR spectra of CBZ, SC, LDH and CBZ-LDH composites.

Figure 4 TEM images of a) pristine LDH, **b)** LDH-CBZ, **c)** LDH-CBZ-SC60(IE) and **d)** LDH-CBZ-SC60. **e)** Diameter of LDH in different samples measured from TEM images.

Figure 5 TG curves and DTG of composites.

Figure 6 *In vitro* CBZ release profiles in **a)** SBF, pH 7.4 and **b)** acetate buffer, pH 4.8. CBZ solution in the respective mediums was used as reference (mean ± SD, n = 3).

Figure 7 Fitting of the data of CBZ release from LDH-CBZ composite to parabolic diffusion (**a** and **d**), pseudo-first (**b** and **e**) and pseudo-second (**c** and **f**) order kinetics for SBF, pH 7.4 **(a-c)** and acetate buffer, pH 4.8 **(d-f)**.

Table 1 CBZ loading and encapsulation efficiency in the different composites.

Table 2II Statistical analysis of CBZ release profiles. Comparisons were made for each system developed with respect to the free drug.

Table 3 Equations for fitting the data of the CBZ release.

Table 4 Correlation coefficient (R2) obtained by fitting the data of the CBZ release into SBF (pH 7.4) and acetate buffer (pH 4.8).

Data availability

No datasets were generated or analyzed during the current study.

Figures

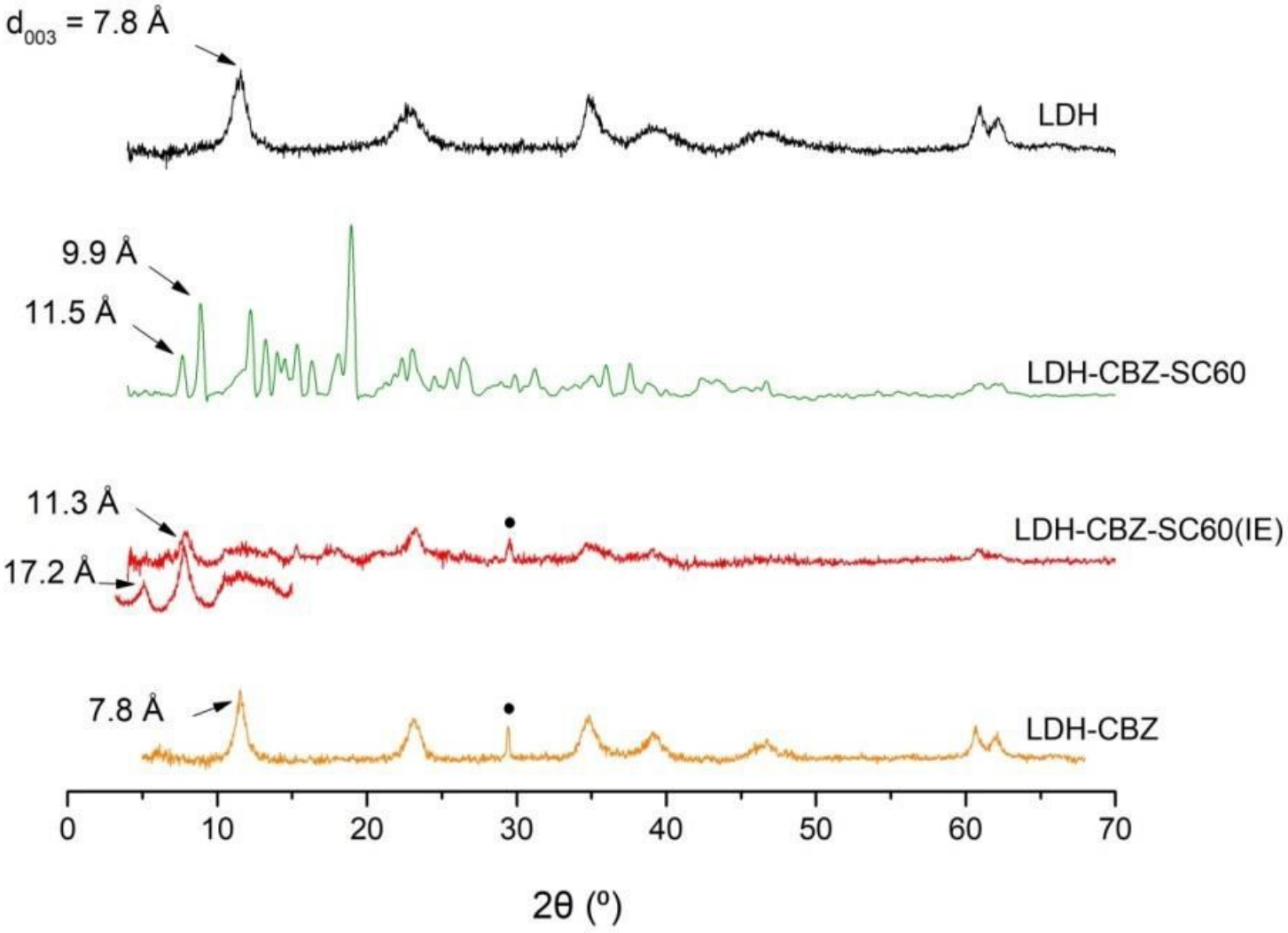

Figure 1

Powder X-ray diffraction patterns of LDH and CBZ-LDH composites. ▯ Indicates peaks of sodium nitrate salt that remains in the sample.

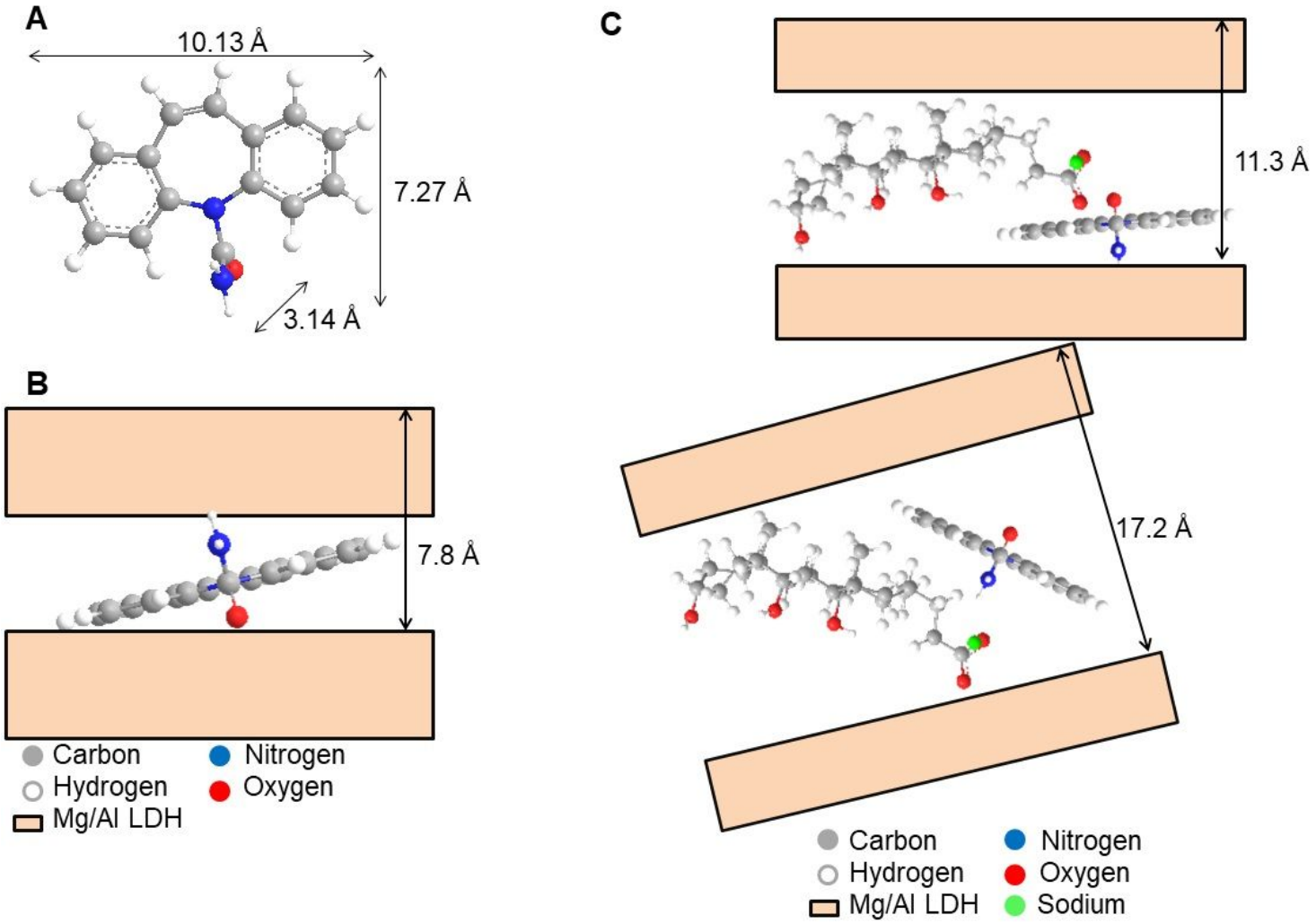

Figure 2

a) CBZ dimensions calculated with Chem3D. b) Probable CBZ orientation in LDH-CBZ. c) Probable CBZ and SC orientation in LDH-CBZ-SC60(IE).

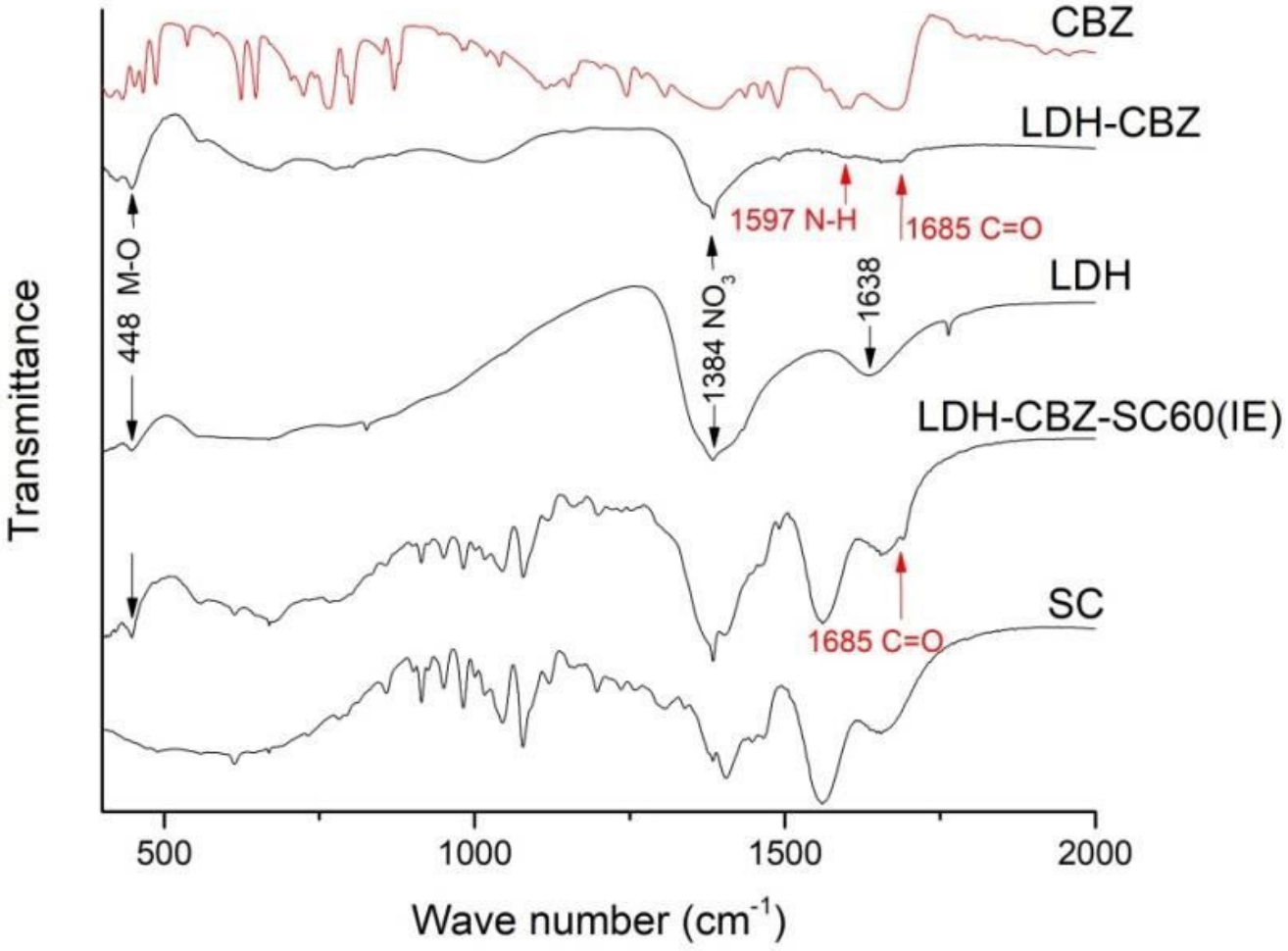

Figure 3

FTIR spectra of CBZ, SC, LDH and CBZ-LDH composites.

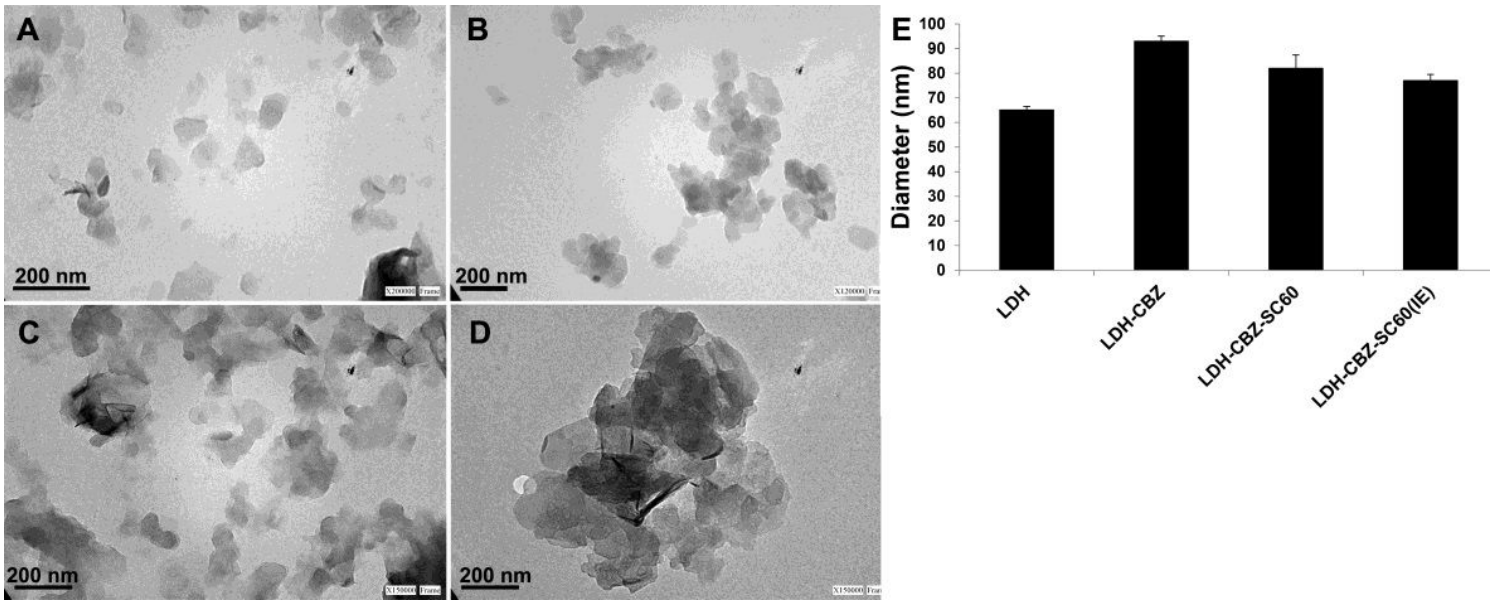

Figure 4

TEM images of a) pristine LDH, b) LDH-CBZ, c) LDH-CBZ-SC60(IE) and d) LDH-CBZ-SC60. e) Diameter of LDH in different samples measured from TEM images.

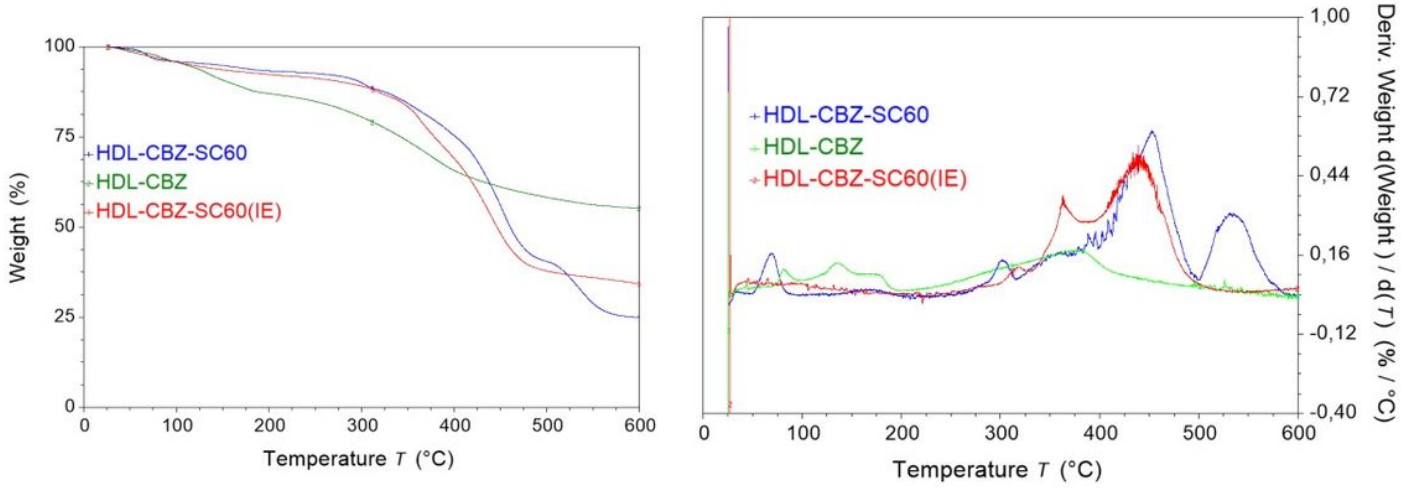

Figure 5

TG curves and DTG of composites

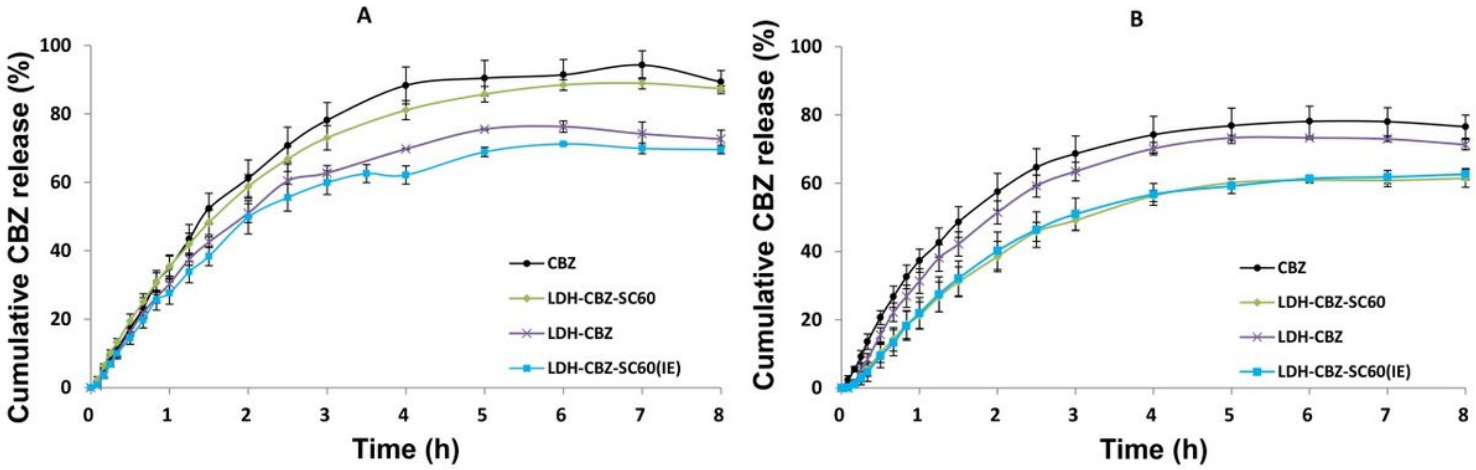

Figure 6

In vitro CBZ release profiles in a) SBF, pH 7.4 and b) acetate buffer, pH 4.8. CBZ solution in the respective mediums was used as reference (mean ± SD, n = 3).

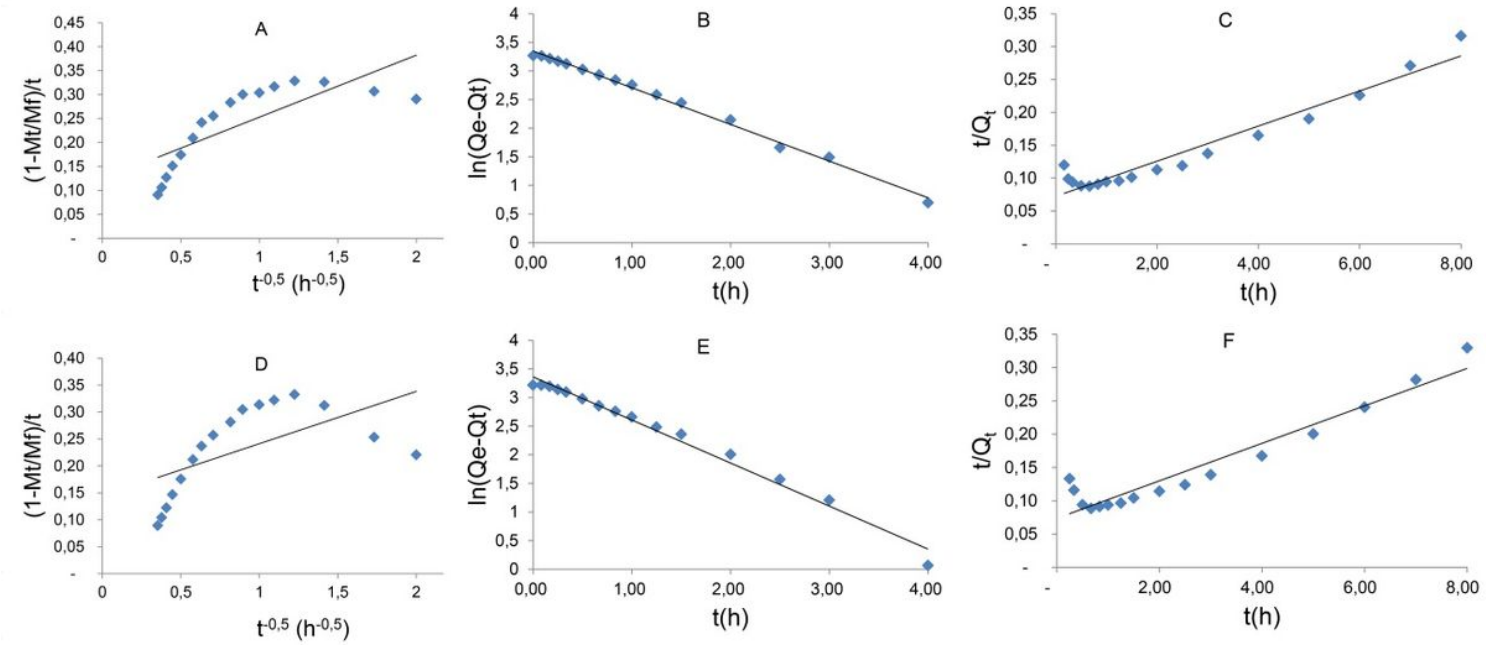

Figure 7

fitting of the data of CBZ release from LDH-CBZ composite to parabolic diffusion (a and d), pseudo-first (b and e) and pseudo-second (c and f) order kinetics for SBF, pH 7.4 (a-c) and acetate buffer, pH 4.8 (d-f).